

Cr–Zr-armalcolite-bearing lamproites of Cancarix, SE Spain

SIMONA CONTINI, GIANPIERO VENTURELLI, LORENZO TOSCANI

Istituto di Petrografia Università, viale delle Scienze, 43100 Parma, Italy

SILVIO CAPEDRI

Istituto di Mineralogia e Petrologia Università, via S. Eufemia, 41100 Modena, Italy

AND

MARIO BARBIERI

Dipartimento di Scienze della Terra, Università 'La Sapienza', Piazzale A. Moro, 00185 Roma, Italy

Abstract

Lamproites with high MgO, high SiO₂ affinity are abundant only in SE Spain where the Cancarix outcrop (in the province of Albacete) occurs. The rocks of Cancarix are peralkaline, saturated to oversaturated in silica, very high in K₂O, Th and *LREE*. The mineralogy and petrography show some variations which depend on the conditions of emplacement and rate of cooling of the magma. The following phases may be present: olivine, phlogopite, K-amphibole, clinopyroxene, sanidine, orthopyroxene, apatite, and, in minor amounts, Cr-spinel, minerals of the pseudobrookite group, ilmenite, roedderite, dalyite, carbonate, analcime (probably pseudomorphous on leucite), a silica phase, rutile, pyrochlore (?), britholite (?) and glass. The lamproites of Cancarix contain Cr–Zr-armalcolite, which is typical of lunar basalts and which has been found also in kimberlites. The composition of early magmatic spinel and the occurrence of Cr–Zr-armalcolite indicate low oxygen fugacity for the primitive magma and related mantle source, in agreement with recent experimental data on lamproitic systems. The redox conditions changed during crystallisation, leading to increase of the Fe³⁺/Fe²⁺ ratio in the system. During the later stages of crystallisation, the residual melts/fluids were depleted in alumina and enriched in several components, e.g. Na, Zr, Fe, *REE*, Cl, etc. stabilising Na-Fe-clinopyroxene, dalyte, arfvedsonitic rims around K-richterite and other alumina-free phases which, on a chemical basis, have been identified as britholite and pyrochlore. Rough comparison with experimental systems and the geochemistry of the rocks suggests that the magma was generated at shallow depth (<<20 kbar) in the lithospheric mantle, which, after early depletion, underwent strong enrichment in many 'incompatible' elements.

KEYWORDS: lamproitic magma, oxygen fugacity, crystallisation, Cancarix, SE Spain.

Introduction

IN SE Spain, the lamproitic rocks occur in the provinces of Murcia, Almeria and Albacete (cf. Venturelli *et al.*, 1984a, 1988), and are penecontemporaneous with a calcalkaline/shoshonitic magmatism of complex origin (crustal anatexis + mantle anatexis). Typical peralkaline lamproites (Calasparra, Las Minas de Hellin, Cancarix, Jumilla) were emplaced to the west of the Carboneras-Palomares-Alhame de Murcia fault system on a crust about 40 km thick ('Meseta-type' crust: De Larouzière *et al.*, 1988). Ultrapro-

tassic rocks with lamproitic affinity, which, cannot however be considered lamproites *sensu stricto*, e.g. Zeneta, Vera and Mazarron occur to the east of this fault system on less than about 25 km thick crust ('Cartagena-type' crust) characterised by high present-day heat flow ($\approx 95 \text{ mW m}^{-2}$) and late Miocene anatectic processes. In this area the rocks with lamproitic affinity show evidence of interaction between lamproitic and calcalkaline/shoshonitic magmas (Venturelli *et al.*, 1984a, 1991a).

The unusual and extreme high-SiO₂, high-MgO character of many Spanish lamproites (Calas-

parra, Las Minas de Hellin, Fortuna, Cancarix) has been related to the strong refractory nature of the mantle, the shallow depth of melting, and the role of H₂O (Foley and Venturelli, 1989). However, these rocks have not been investigated in detail yet, and little is currently known on the magmatic evolutionary processes. This paper reports chemical and petrographic data on the lamproites from Cancarix which are peculiar in many respects: besides high SiO₂ and MgO they contain Cr–Zr-armalcolite, much-reduced Cr-spinel and unusual Al-free minerals which formed at the late stage of the crystallisation.

Petrographic and mineralogical outlines

The outcrop of Sierra de las Cabras near Cancarix (province of Albacete) was formerly described by Gomez de Larena (1934) and Hernandez-Pacheco (1965), and more recently by several authors (Fuster *et al.*, 1967, and Venturelli *et al.*, 1988, for detailed references).

The outcrop covers an area of about 0.7 km² and rises up to 60 m over the surrounding plain (Fig. 1). According to the remains of the eroded volcanic body, the emplacement of the magma occurred apparently in two steps: (1) opening of the volcanic conduit through Mesozoic sediments (mostly limestone and dolomite) which were fragmented, rounded and intercalated to glassy magmatic rocks, hereafter referred as 'external lamproites'; these lamproites are sometimes scoriaeous and constitute a funnel-shaped extrusive and dyke-like sequence; (2) emplacement of new magma protruding through the 'external lamproites'; it generated the main part of the outcrop hereafter referred as 'main body', which is characterised by polygonal joints. The main body is interpreted by Mitchell and Bergman (1991) as a lava lake. The age of the rock is about 7.5 Ma (K/Ar data on sanidine and K-richterite: Nobel *et al.*, 1981).

The 'external lamproites' are petrographically strongly variable. Glassy types contain mostly phenocrysts of olivine (which includes Cr-spinel), phlogopite, clinopyroxene and apatite; varieties with accessory glass contain sanidine in addition. The rocks of the 'main body' are holocrystalline (grain size up to 1 mm) and consist of sanidine, K-rich amphibole, olivine, phlogopite, clinopyroxene, apatite, orthopyroxene in decreasing abundance, accessory Cr-spinel (mostly included in olivine), ilmenite, roederite (abundant in some samples), Na-clinopyroxene, a silica phase, dalyte, late magmatic carbonates, rutile and other minerals which, on the basis of their chemistry, have been referred to as britholite and pyro-

chlore. All the rocks may contain minerals belonging to the pseudobrookite group. Data on mineral phases—reported in Tables 1–4—have been obtained by a microprobe ARL-SEM-Q at 15 kV, 20 nA, and by an electron microscope JEOL 6400 equipped with TRACOR EDS-microanalysis at 15 kV, 0.62 nA.

Unaltered *olivine* contains small crystals of Cr-spinel, which are typical of all Spanish lamproites. Mg# (up to 94) decreases with the size of the crystals.

Phlogopite occurs as (i) unstable saenitic crystals with cores rich in magnesium Mg# ≈ 93) and chromium (up to 1.4 wt.% Cr₂O₃), and moderately low in titanium (1.7 wt.% TiO₂); (ii) sieve-textured crystals which include droplets of colourless glass; (iii) euhedral to anhedral F-rich (up to 5.1 wt.%) phenocrysts of variable size; (iv) small, deeply coloured euhedral microliths very rich in titanium and iron occurring in a glassy matrix; (v) reaction coronas around olivine phenocrysts, (vi) rounded deep-brown crystals rich in fluid-melt inclusions and poikilitically included in K-feldspar and K-amphibole.

K-richterite—formerly identified by Hernandez-Pacheco (1965)—is the main mafic phase in the rocks of the main body. It is pleochroic from yellow to purple-brownish, contains abundant fluorine (up to 2.0 wt.%) and develops arfvedsonitic rims enriched in sodium and iron. Frequently amphibole mantles olivine, phlogopite, and (?) roederite as reaction product.

Two types of *clinopyroxene* have been detected. (i) Small (<0.25 μm) diopside crystals (Mg# 91) with very low titanium (0.6–0.8 wt.% TiO₂) and aluminium (0.27–0.65 wt.% Al₂O₃); (ii) very small Na-Fe-rich (up to 11 wt.% Na₂O, Mg# down to 17) late-clinopyroxene occurring only in holocrystalline rocks (Fig. 2a).

Orthopyroxene (Mg# 55–86) mostly occurs as anhedral crystals of variable size, sometimes zoned with rims enriched in iron and manganese; more rarely as reaction coronas around olivine.

Fe-rich *sanidine* (up to 3.6 wt.% Fe₂O₃) varies in modal proportions (0–60% vol.) and increases with the crystallinity of the rocks; in low crystallinity samples, sanidine may occur in radial aggregates, whereas in the holocrystalline samples it occurs as large poikilitic laths including clinopyroxene, apatite and rare phlogopite.

Analcime is sporadic in glassy lavas where it occurs as rounded, globular microlites.

Apatite forms prismatic crystals of variable size (up to 100 μm) frequently enclosed in sanidine; its fluorine content is high (1.65–2.65 wt.%) and REE largely variable (La₂O₃ ≈ 0.27–0.65, Ce₂O₃ ≈ 0.76–1.1, Nd₂O₃ ≈ 0.44–0.068, Sm₂O₃ ≈ 0.1–

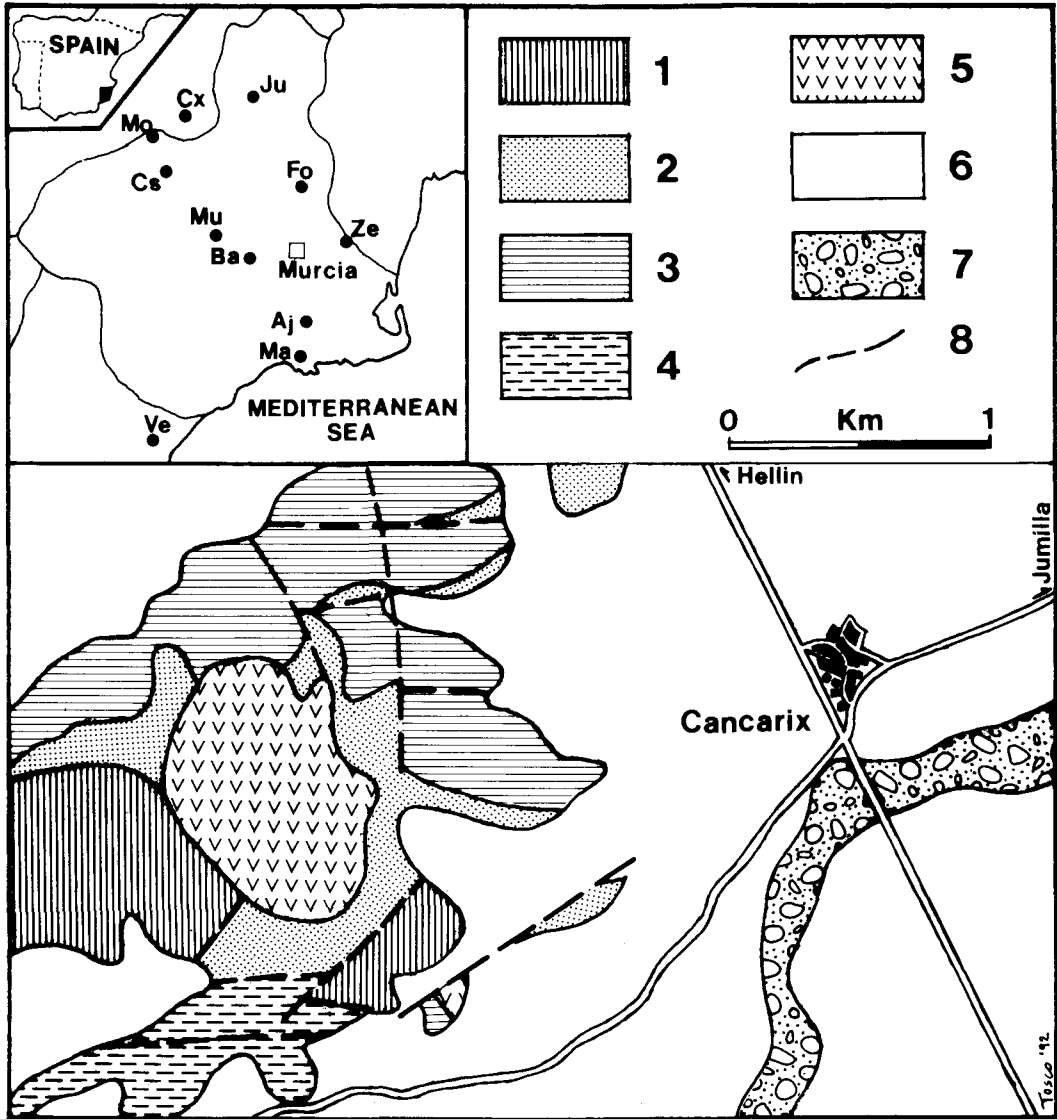


Fig. 1. Sketch map of the Cancarix outcrop (modified after Mapa Geologico de España IGME, Hoja 686 Issa). 1, Dolomites and massive oolitic limestone (Dogger); 2, Marls and marly limestones (Early Malm); 3, Light-brown dolomites (Middle Malm); 4, White dolomites and dolomitic mudstones (Late Cretaceous); 5, Lamproites; 6, Sediments of prevalent continental origin (Quaternary); 7, Recent fluvial sediments; 8, Faults. Inset: locations of lamproites and ultrapotassic rocks with lamproitic affinity. Ju = Jumilla, Cx = Cancarix, Mo = Las Minas de Hellin, Cs = Calasparra, Mu = Puebla de Mula, Ba = Barqueros, Ze = Zeneta, Aj = Aljorra, Ma = Mazarron, Ve = Vera.

0.2 wt.%). Very late apatite (Fig. 2b) may be enriched in chlorine (up to 1.1 wt.% Cl).

Cr-spinel (40–67 wt.% Cr₂O₃) is frequently included in olivine as small deep-brown euhedra.

Ilmenite occurs as anhedral to subhedral unmixed crystals. Overall compositions indicate

high chromium content (≈ 1.2 wt.% Cr₂O₃) which suggests early crystallisation or a xenocrystic origin.

Different varieties of minerals of the *pseudobrookite* group (Bowles, 1988) are present: (i) homogeneous armalcolite–pseudobrookite; (ii)

homogeneous Cr–Zr-armalcolite (up to 6 wt.% Cr₂O₃, up to 3.6 wt.% ZrO₂) in the form of very small crystals (≈20 μm) with slight variation of the FeTi₂O₅/Ti₃O₅ mole ratio (Fig. 3).

Hernandez-Pacheco (1965) described an unidentified blue-pleochroic mineral which may now be regarded as *roedderite*. Roedderite belongs to the osumillite subgroup (Abraham *et al.*, 1983: general formula $W_{1-2}X_2Y_3Z_{12}O_{30}$, where $W = K, Na$; $X = Mg, Fe^{2+}$; $Y = Mg, Fe^{2+}, Al, Fe^{3+}$; $Z = Si, Al$) and is almost alumina-free. The roedderite occurs in Cancarix lamproites (i) as small blue to colourless anhedral crystals in coarse grained rocks or (ii) as very late pale blue laths mainly in veinlets crossing the groundmass of some external lavas. Optical and microprobe analysis indicate that the roedderite has variable Mg/Fe ratio and Na₂O content. Iron occurs mainly in the trivalent state (M. F. Brigatti, pers. comm., 1992) and is highest in type (i), which has a composition close to the chayesite end-member (Velde *et al.*, 1989).

Dalyte—a mineral already described at Cancarix by Linthout *et al.* (1988)—crystallised late, sometimes contemporaneously with a silica phase and arfvedsonitic amphibole (Figs. 2b, c), and exhibits variable TiO₂/ZrO₂ weight ratio (0.03–0.37). This mineral is an alkali-zirconosilicate which represents the Zr-rich end-member of the dalyte–davanite [K₂(Zr,Ti)Si₆O₁₅] series.

Very small anhedral crystals (up to 20 μm), sometimes occurring in microvugs, identified by SEM, are probably *britholite* [A₅(BO₄)(OH,F), where A = Ca, REE, Na, U, Th, Pb and B = Si, P] (Fig. 2a) and *pyrochlore* [A_{2-m}B₂O₆-(OH,F)_{1-n}, where A = Na, Ca, K, Mg, Mn, Pb, REE, Sr, Th, U, Y, and B = Nb, Ta, Ti, V]. The

different crystals of britholite have widely variable composition (e.g. SiO₂ ranges from 0 to 13.3 wt.%) probably related to the substitution Ca + P = REE + Si. Pyrochlore shows little replacement of Ti in site B, where Nb is the main cation; U and Th are the most abundant components in site A so that, according to Hogarth (1977), it may be classified as uranpyrochlore.

A TiO₂ phase, possibly *rutile*, sometimes occurs in association with roedderite.

A silica phase may fill microscopic vugs.

Carbonate may be present in small amounts as a late crystallising phase in holocrystalline rocks.

Geochemistry

The rocks from Cancarix exhibit high K₂O and SiO₂ (up to 9.5 and 57.9 wt.% respectively in unaltered samples: Table 5). No significant compositional variations have been detected within the outcrop, excluding potassium depletion and sodium enrichment in some altered glassy varieties. The rocks are saturated to oversaturated in silica and have high agpaitic index [(Na + K)/Al, atomic ratio, mostly in the range 1.1–1.3]. The samples have comparable REE contents (Table 6) and LREE-enrichment (Ce_N/Yb_N = 37.0–45.6), and show typical 'Mediterranean' REE pattern (cf. Foley *et al.*, 1987) having low La/Nd ratio (0.54–0.60). Moreover, the rocks exhibit a small negative Eu anomaly (Eu/Eu* ≈ 0.7) which is also typical of the potassic-ultrapotassic rocks of the western Mediterranean area.

Strontium isotope data on bulk rocks (Table 7) have been obtained by a VG Micromass 54E spectrometer on samples dissolved in HF +

Table 1. Representative analyses of olivine, orthopyroxene and clinopyroxene from the Cancarix lamproites.

	Olivine				Orthopyroxene				Clinopyroxene			
	718e L	719b L	720b M	725b S	725b	725b core rim		725b	701e	664bz	725b very late	
SiO ₂	40.20	41.60	39.60	40.20	56.60	56.70	52.60	56.10	53.80	54.30	52.30	52.20
TiO ₂					0.20	0.17			0.57	0.82	0.79	1.01
Al ₂ O ₃									0.27	0.32		
FeO _{tot}	5.75	7.65	14.90	17.40	8.95	12.40	26.20	9.88	3.31	4.32	13.60	24.90
MnO			0.18	0.55	0.33	0.23	0.80	0.33	0.13	0.14		0.20
MgO	52.60	50.40	45.30	42.50	32.00	30.50	20.30	32.00	19.40	18.20	10.80	3.47
CaO	0.06	0.08	0.10	0.19	1.22	0.87	0.23	1.16	22.10	21.10	14.00	5.73
NiO	0.57	0.52	0.32									
Na ₂ O									0.24	0.25	4.86	10.20
Cr ₂ O ₃					0.12	0.19		0.32	0.53	0.44	0.79	
Total	99.18	100.26	100.40	100.84	99.42	101.06	100.13	99.79	100.35	99.89	97.14	97.71
Mg#	94.2	92.2	84.4	81.3	82.0	81.4	58.0	85.2	91.3	88.2	58.5	19.9

e, bz, b = external lamproites, border zone of the main body and main body respectively.

L, M, S = large, medium and small crystals.

Mg# = 100 Mg/(Mg+Fe) atoms

Table 2. Representative analyses of phlogopite, K-amphibole, roedderite and sanidine from the Cancrax lamproites.

	Phlogopite						K-Richterite						Roedderite				Sanidine			
	664bz		724b		725b		719b		724b		725b		718e		719b		719b		725b	
	type (v)		type (v)		type (v)		type (i)		type (i)		type (v)		in microveins		in microveins		in microveins			
	core	rim	core	rim	core	rim	core	rim	core	rim	very late	rim	rim	rim	rim	rim	rim	rim	rim	rim
SiO2	41.20	40.50	40.40	40.30	41.80	40.40	40.20	53.60	53.10	53.70	52.70	52.00	69.50	69.90	69.10	67.50	62.60	65.50		
TiO2	3.96	6.44	8.35	1.70	2.35	8.57	8.31	3.97	7.15	6.60	8.40	6.37	0.17	0.37	0.25	0.11				
Al2O3	11.20	10.80	10.10	13.00	11.70	9.89	10.50	0.79	0.27				0.09	0.21	0.17	0.05	17.80	17.50		
FeO	3.77	6.16	6.16	2.62	3.49	6.24	6.02	3.15	6.22	12.80	15.30	20.10	6.64	5.77	12.00	13.90	1.41	1.18		
MnO	0.01	0.03	0.06		0.04	0.04	0.01	0.08	0.17				0.15	0.13	0.30	0.27	0.06	0.02		
MgO	24.30	21.10	19.90	26.10	24.90	18.90	19.80	20.60	16.30	12.00	9.04	6.63	15.70	16.40	11.30	10.40	0.05	0.02		
CaO	0.02	0.05			0.04			7.00	5.76	3.84	2.47	1.12			0.01		0.02			
Na2O	0.27	0.30	0.43	0.34	0.12	0.09	0.16	4.34	4.54	5.49	6.17	6.82	0.97	1.35	0.53	0.60	0.65	0.39		
K2O	10.00	9.76	9.63	10.00	10.00	9.55	9.28	3.75	4.00	3.68	4.37	4.34	4.49	4.59	4.42	4.24	16.20	15.50		
BaO							0.37										n.d.	0.26		
Cr2O3	0.31	0.39	0.30	1.22	1.03	0.50	0.32	0.02	0.13											
F	5.09	3.31	2.41	n.d.	2.11	0.95	1.62	1.99	0.85	n.d.	n.d.	n.d.								
Total	100.13	98.84	97.74	95.28	97.54	95.13	96.59	99.29	98.49	98.11	98.57	97.83	97.51	98.72	98.08	97.07	98.74	98.79	100.37	
Mg#	92.0	85.9	85.2	94.7	92.7	84.4	85.4	92.1	82.4	62.6	51.3	37.0	80.80	83.50	62.70	57.10	85.7			

n.d. = not determined

Table 3. Representative analyses of spinel included in olivine, pseudobrookite type minerals and ilmenite from the Cancarix lamproites.

	Spinel				Cr-Zr-Armalcolite		Armalcolite-Pseudobrookite				Ilmenite
	701e	678e	678e	720b	725b	725b	669e	719b	724b	725b	725b
TiO ₂	1.36	1.53	1.35	6.80	67.68	70.20	66.96	67.40	59.00	55.80	52.10
Al ₂ O ₃	2.95	3.02	2.81	0.11			0.41		0.04		
Cr ₂ O ₃	61.40	59.70	58.20	42.70	5.28	4.92	1.00	0.61	0.43	0.69	1.23
Fe ₂ O ₃	2.10	2.84	4.64	13.80			9.02	10.60	19.30	24.10	0.67
FeO	27.80	26.60	22.53	34.20	18.26	18.00	10.92	12.80	15.10	13.20	39.45
MnO	0.45	0.66	0.60	0.66	0.23		0.11	0.13	0.75	0.69	0.63
MgO	3.52	3.96	6.10	2.11	3.06	1.81	9.27	8.36	3.46	3.19	3.32
CaO					1.32	1.31	0.14		0.05		
ZrO ₂					2.34	2.55	0.10	0.10	0.10	0.24	
Total	99.58	98.31	96.23	100.38	98.17	98.79	97.93	100.00	98.23	97.91	97.40

Fe₂O₃ calculated on the basis of O=4 and cations = 3 for spinel, according to Bowels (1988) for armalcolite-pseudobrookite and on the basis of O = 3 and cations = 2 for ilmenite.

HClO₄ + H₂O mixture. The ⁸⁷Sr/⁸⁶Sr ratio for SRM 987 standard was 0.71022. The initial ⁸⁷Sr/⁸⁶Sr ratios for the external lamproites are in the range 0.71695–0.71733, the lowest value characterizing the analcime-bearing type; for the rocks of the main body, the ratio covers a very narrow range 0.71732–0.71739. A very low value of ¹⁴³Nd/¹⁴⁴Nd (0.51125) has been reported by Nelson *et al.* (1986) for the rocks of the main body.

Conditions of crystallisation

Oxygen fugacity. Assuming that the composition of spinel remained unchanged after magma crystallisation, the Fe³⁺/Fe²⁺ ratio in the parent

melt may be evaluated using the spinel-liquid distribution coefficient obtained by Foley (1985) for lamproitic systems. Furthermore, using the obtained Fe²⁺/Fe³⁺ ratios of the melt and extrapolating to lamproitic compositions the equation proposed by Kilinc *et al.* (1983), the oxygen fugacity may be estimated at different temperatures. Although all the rocks of Cancarix have very similar composition, the *f*_{O₂} values calculated using Cr-spinel included in olivine are variable from place to place. The highest values have been found for the main body (≈QFM + 0.2 log unit), the lowest for the external lamproites (≈IW + 0.6–2.7 log unit). It is noteworthy that the lowest value has been obtained for a very well preserved glassy sample. The different conditions of redox are probably related to different conditions of crystallisation. The high rate of crystallisation of the external lamproites 'froze' the olivine and Cr-spinel compositions, which thus reasonably reflect the intensive parameters of the magma at depth; on the contrary, the slower crystallisation of the main body possibly favoured partial reequilibration of these phases under increasing oxidation conditions. Oxidation of the magma may be due to dissociation of water and to a semipermeable membrane behaviour of the magma with consequent retention of oxygen and loss of hydrogen from the cooling magmatic body. Note that less than 0.1 wt.% H₂O dissociation is sufficient for oxidation from IW to QFM (Foley *et al.*, 1986a, and references therein).

In spite of the different redox conditions evidenced by Cr-spinel, both external lamproites and main body may contain Fe³⁺-bearing armalcolite/pseudobrookite and Cr, Zr, Ti³⁺-bearing armalcolite. The last mineral is typical of strongly

Table 4. Representative analyses of dalyte, britholite (?) and pyrochlore (?) from Cancarix lamproites.

	Dalyte		Britholite*	Pyrochlore*
	725b	725b	725b	725b
SiO ₂	63.60	64.20	13.3	1.7
TiO ₂	1.08	4.65		6.4
Al ₂ O ₃			4.0	
FeO†	0.84	0.17	0.2	2.9
MgO	0.36	0.17	1.4	0.2
CaO	0.23		3.0	2.5
Na ₂ O			0.2	1.9
K ₂ O	15.20	16.70		
P ₂ O ₅			13.4	
Nb ₂ O ₅				42.5
ZrO ₂	18.00	13.30		
ThO ₂			16.2	19.6
UO ₂			10.7	22.8
La ₂ O ₃			6.5	
Ce ₂ O ₃			21.2	
Nd ₂ O ₃			10.4	
Total	99.31	99.19	100.5	100.5

*. Semiquantitative analysis

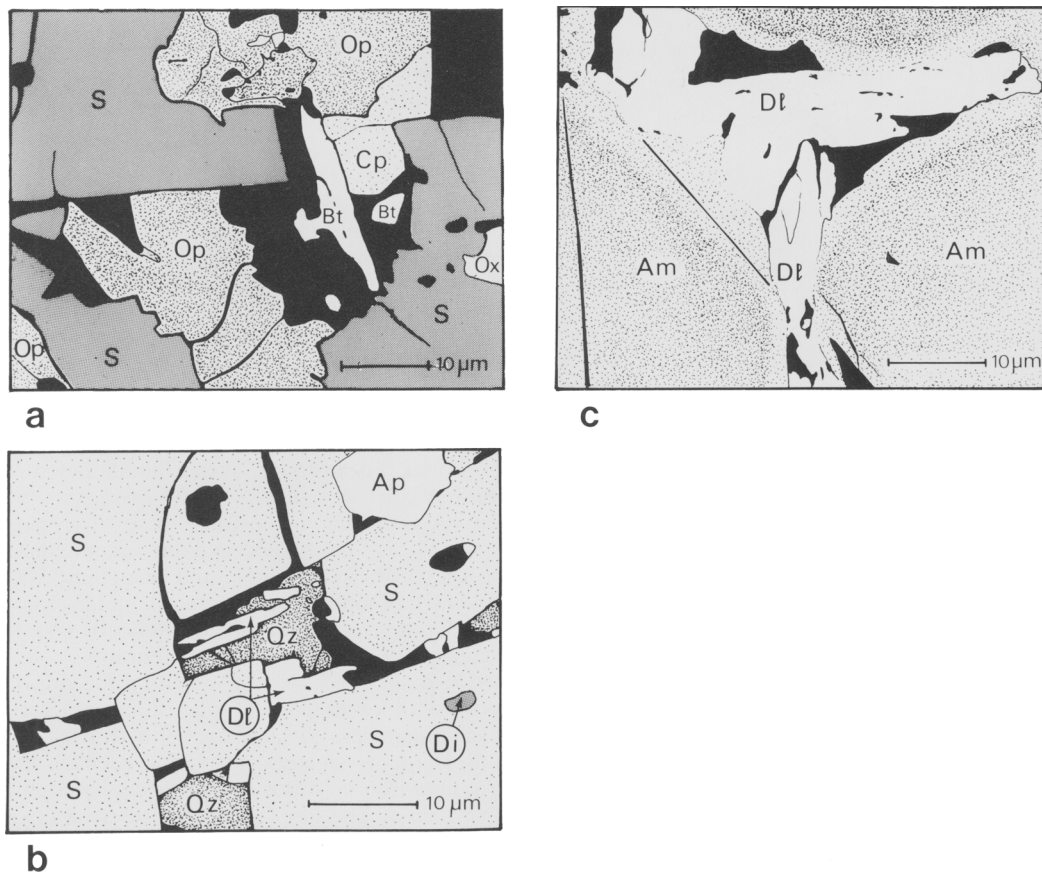


FIG. 2. (a) Presumed britholite (Bt) coexisting with very late Na-Fe-clinopyroxene (Cp); Op = orthopyroxene, S = sanidine, Ox = oxide. (b) Very late dalyte (Dl) and a silica phase (Qz); Di = diopside, S = sanidine, Ap = late apatite. (c) Dalyte (Dl) crystallised close to Na-enriched arfvedsonitic rims of zoned K-amphibole (Am).

reduced lunar rocks (cf. Bowles, 1988, and references therein) and is also present in kimberlites (Haggerty, 1987, and references therein) mostly as xenocrysts. According to the experimental data obtained by Friel *et al.* (1977), Fe^{2+} -Mg armalcolite ($\text{Fe}_{0.5}\text{Mg}_{0.5}\text{Ti}_2\text{O}_5$) at 1200°C is stable from $10^{-9.5}$ to $10^{-10.5}$ atm f_{O_2} . Below $10^{-10.5}$ atm f_{O_2} , a reduced Ti^{3+} -bearing armalcolite appears. The occurrence of strongly reduced Cr-Zr-armalcolite in the rocks of Cancarix may be explained theoretically in three different ways. (i) Cr-Zr-armalcolite represents a late phase crystallised from local domains with low oxygen fugacity; redox heterogeneity has been suggested, for instance, by Yeremeyev *et al.* (1988) to explain flakes of native metals in a lamproite from Central Aldan. Cr-Zr-armalcolite represents (ii) an early magmatic or (iii) a mantle-derived phase which was occasionally preserved even in the relatively oxidised main body of Cancarix. We

think that hypothesis (ii) is more reliable for the following reasons: (a) the mineral is rich in chromium, in agreement with crystallisation from a chromium-rich environment; (b) it has rather constant composition suggesting crystallisation under almost constant f_{O_2} , a condition which should be very difficult to realise in the different microenvironments supposed by hypothesis (i); (c) the mineral does not exhibit unequivocal evidence of xenocrystic nature.

Crystallisation of the different lamproitic facies. The outcrop of Cancarix exhibits three different rocks facies which underwent different conditions of emplacement and crystallisation; (a) vitreous to glass-bearing external lamproites ('black lavas' of Hernandez-Pacheco, 1965) emplaced very close to the surface (possibly giving lava flows also, which are now eroded) and containing small olivine and phlogopite phenocrysts; (b) hypocrySTALLINE rocks forming the border zone of the main

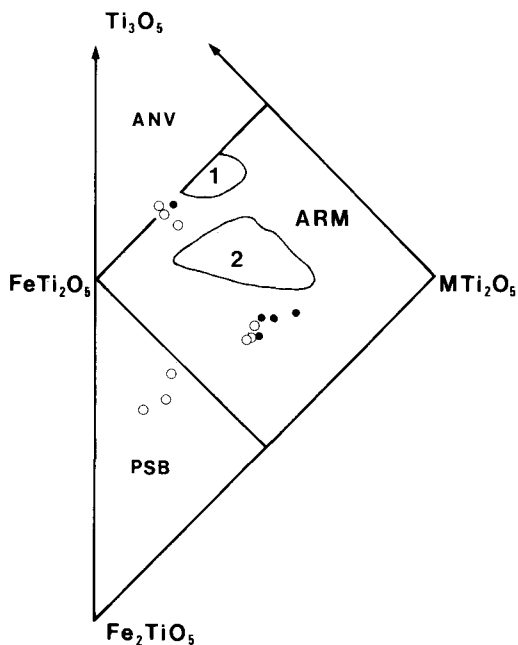


FIG. 3. Pseudobrookite group minerals: dot = external lamproites, circle = main body. ANV = anosovite, ARM = armalcolite, PSB = pseudobrookite, M = Mg, Mn, Ca; 1, field of Cr-Zr-Ca lunar armalcolite; 2, field of lunar armalcolite. Cr-Zr-armalcolite from Cancarix falls around the anosovite-armalcolite boundary. End-member calculation and classification according to Bowles (1988)

body, characterised by the presence of phlogopite microcrysts; (c) holocrystalline rocks constituting the main lamproite body, characterised by K-richterite as a main femic phase.

In group (a), different steps of crystallisation may be recognised. Vitreous rocks contain only olivine, Cr-spinel and euhedral to anhedral phlogopite type *iii* phenocrysts, whereas rocks with higher degree of crystallinity also exhibit apatite and pyroxene microphenocrysts.

Group (b) contains olivine, Cr-spinel, phlogopite phenocrysts type *iii*, phlogopite type *iv* microphenocrysts, sanidine, clinopyroxene and apatite.

The rocks constituting the main body (group c) probably represent the product of crystallisation of a single magma batch. Sanidine (≈ 50 vol.%) and K-richterite are the most abundant phases. Olivine, phlogopite, clinopyroxene and also roederite reacted frequently with the liquid generating K-amphibole. The reaction forsterite + roederite + diopside + melt + vapour \rightarrow richterite occurring at decreasing temperature under H_2O -

saturated conditions has been investigated experimentally by Charles (1975); the reaction phlogopite + melt \rightarrow K-richterite has been described previously by Best *et al.* (1968) in the lamproite occurring at Moon Canyon (Utah).

In all groups, olivine may exhibit reaction coronas of phlogopite type *v* and of orthopyroxene.

The analcime origin and related problems. As described in the petrographic section, some lava samples contain isotropic analcime as small crystals (up to 0.03 mm) set in the glassy matrix. The origin of analcime in lavas and hypabyssal rocks is still a matter of debate, but, in our opinion, there is no evidence of its strictly magmatic origin (cf. Karlsson and Clayton, 1991). Analcime has been found also in other Spanish lamproites. For instance, in the Jumilla outcrop, iron-rich analcime (Fe_2O_3 up to 1.6–1.9 wt.%) may be abundant in the form of small crystals occurring in the holocrystalline groundmass together with K-amphibole and phlogopite. On the basis of optical, geochemical and isotopic considerations, this analcime was related to Na-K exchange reaction on leucite (Venturelli *et al.*, 1991b, p. 135 and 140) as shown by the drastic decrease of the K_2O/Na_2O ratio in the analcime-bearing samples, the scattered Rb distribution and the rough negative correlation between the strontium-isotope ratios and the modal amounts of analcime. The last feature indicates input of radiogenically depleted Sr from the surrounding carbonate sediments.

Actually, the analcime-bearing rocks from Cancarix exhibit a notable increase in Na_2O , Cl and Rb (which is negatively correlated with K_2O), a moderate increase of Y, a decrease of K_2O and total alkalis, and a small but significant decrease of the Sr-isotope ratio (Table 7). These features support a secondary origin for analcime after original leucite (or glass) reacting with fluids carrying components coming from the surrounding carbonate sediments, as suggested by the lower strontium-isotope ratio. The mobility of Y may be related to the formation of complexes with alkalis and halogens (Mineyev, 1963).

The preservation of ferro-magnesian minerals could argue against a secondary origin of analcime. The absence of alteration of these minerals, however, may be explained by (i) slow reactions with fluids and (ii) overlapping of the stability temperature of analcime and ferro-magnesian minerals. The reaction of $KAlSi_2O_6$ leucite + Na^+ solution + H_2O = $NaAlSi_2O_6 \cdot H_2O$ analcime + K^+ solution proceeds very rapidly even at moderate temperature (the activation energy is about 6–20 Kcal mole $^{-1}$ at 150–225 °C), whereas alter-

ARMALCOLITE-BEARING LAMPROITES

Table 5. Major and trace element composition of the Cancarix lamproites.

	678e	681e	691e	693e	709e	712e	716e	717e	718e	664bz	688bz	719b	720b	721b	722b	723b	724b	725b
SiO ₂	56.82	57.84	56.54	58.51	56.61	56.29	56.65	56.94	57.86	56.90	57.21	57.49	57.17	56.89	56.50	57.81	56.71	55.92
TiO ₂	1.54	1.56	1.54	1.60	1.55	1.56	1.53	1.54	1.57	1.54	1.55	1.57	1.55	1.56	1.51	1.58	1.51	1.49
Al ₂ O ₃	9.69	9.82	9.55	10.03	9.69	9.81	9.69	9.40	9.81	9.61	9.61	9.72	9.67	9.76	9.50	9.84	9.44	9.30
FeO ^a	4.55	4.64	4.54	4.67	4.55	4.62	4.58	4.55	4.65	4.58	4.63	4.69	4.66	4.71	4.72	4.75	4.73	4.67
MnO	0.07	0.06	0.07	0.06	0.07	0.07	0.07	0.07	0.07	0.07	0.07	0.07	0.07	0.07	0.08	0.07	0.07	0.08
MgO	11.22	9.85	11.50	7.71	11.28	11.41	10.33	11.34	10.20	11.49	11.36	10.97	11.71	11.59	12.23	10.23	11.26	11.79
CaO	3.40	3.15	2.97	3.08	3.29	3.56	3.37	2.98	3.23	3.48	3.34	3.12	3.09	3.20	3.46	3.19	3.62	4.12
Na ₂ O	0.90	0.80	1.50	1.00	2.07	2.93	1.31	1.77	0.91	0.60	0.67	0.91	1.01	0.99	0.96	1.02	1.08	1.08
K ₂ O	8.54	8.96	6.49	9.45	6.13	5.00	8.00	7.01	9.09	8.73	8.79	9.27	9.16	9.15	9.10	9.20	9.12	8.93
P ₂ O ₅	1.11	1.07	1.04	1.08	1.03	1.06	1.09	1.05	1.11	1.08	1.08	1.11	1.13	1.12	1.23	1.18	1.30	1.24
LOI	2.27	2.28	3.96	2.33	3.77	3.72	3.43	3.38	1.18	1.79	1.44	0.81	0.53	0.72	0.54	0.79	0.92	1.22
F	n.d.	n.d.	0.35	0.41	n.d.	n.d.	n.d.	n.d.	0.37	0.37	0.37	0.37	0.37	0.37	0.36	0.39	0.37	0.37
Total	100.11	100.03	100.05	99.93	100.04	100.03	100.05	100.03	100.05	100.14	100.12	100.10	100.12	100.13	100.19	100.05	100.13	100.21
Ni	449	499	421	394	489	469	402	465	454	479	472	511	474	491	479	482	489	493
Co	37	32	32	25	36	33	32	33	35	33	34	34	32	33	37	33	34	34
Cr	680	696	688	731	7	673	681	693	687	685	699	673	713	716	716	687	730	737
V	87	83	83	85	81	85	80	83	82	83	81	83	86	86	83	83	82	82
Sc	11	14	13	13	13	10	13	13	12	13	13	13	15	13	14	13	14	14
Cu	31	34	29	33	34	31	35	28	30	33	35	28	32	32	31	36	35	38
Zn	77	81	78	80	77	79	78	78	83	76	81	76	78	76	75	81	75	79
Ga	26	21	20	23	20	22	21	21	21	23	24	22	22	22	20	22	20	21
Rb	480	589	1135	568	1673	1628	656	877	512	622	617	674	703	670	566	557	538	556
Sr	690	693	662	703	686	685	658	691	693	693	744	738	760	753	837	770	868	816
Ba	2533	1970	1721	1797	1843	1813	1919	1831	2198	2168	2076	1767	1505	1560	2003	1772	2831	1855
Zr	766	845	857	859	839	772	832	873	814	846	897	899	890	883	852	887	823	838
Nb	40	41	42	41	42	42	39	41	40	41	45	46	44	43	45	45	44	45
Y	25	30	47	33	50	48	38	44	29	31	34	31	33	34	34	32	30	33
Pb	79	85	85	67	93	86	82	81	92	81	88	79	97	97	117	90	118	113
Th	131	134	125	128	124	122	123	126	125	125	125	128	131	132	140	133	141	133
Cl			1465	304					263	320	154	185	185	180	196	189	278	229

Major element analyses have been performed by XRF on glass disks; trace elements have been determined by XRF on powder pellets; e, bz, b = external lamproites, border zone of the main body and main body respectively.
 n.d. = not determined
 * determined by IMAA using Ge(Li) coaxial and Ge(Mn) planar detectors.

Table 6. Hf, Ta, U and REE distribution in the Cancarix lamproites.

	691e	693e	668bz	719b	721b	723b	724b	725b
Hf	22.3	23.2	22.7	23.6	22.3	23.4	22.8	22.6
Ta	3.55	4.05	4.18	4.42	4.20	3.72	3.95	3.91
U	25.0	17.0	17.0	13.0	9.00	18.0	18.0	16.0
La	108	109	105	106	112	107	116	109
Ce	297	302	300	300	310	311	319	307
Nd	189	193	195	185	191	191	200	182
Sm	35.3	35.0	36.0	34.2	35.5	35.2	36.3	35.8
Eu	5.48	5.52	5.54	5.59	5.68	5.62	5.80	5.56
Tb	1.91	1.83	1.75	1.66	2.04	1.94	1.65	1.62
Yb	1.87	2.08	1.93	1.91	2.11	1.81	1.78	1.79
Lu	0.22	0.26	0.26	0.23	0.28	0.22	0.23	0.23

Analyses have been performed by NAA using Ge(Li) coaxial and Ge(nl) planar detectors.

ation of olivine to serpentine is slower (cf. Korytkova and Makarova, 1971); thus rapid migration of fluids may prevent olivine transformation. The highest stability temperature for analcime at low pressure is about 400 °C or less, whereas the lowest for olivine (reaction—olivine + water → crysotile + brucite) is about 350–400 °C. Thus, considering the large degree of uncertainty in the experimental data, the contemporaneous stability of analcime and olivine in a small temperature interval is consistent. It is noteworthy, however, that the fluids were carrying at least alkaline elements and olivine would react with them at high temperature generating minerals other than serpentine, e.g. phlogopite. Actually, no reaction coronas are found around olivine in the analcime-bearing rocks. Thus we prefer hypothesis (i).

Main crystallisation path. The composition of the lamproites from Cancarix may be satisfactorily represented in terms of Mg_2SiO_4 – $KAlSiO_4$ – SiO_2 components (≥ 76 wt. % of total composition for samples with L.O.I. ≤ 2 wt. %). The system Mg_2SiO_4 – $KAlSiO_4$ – $SiO_2 \pm H_2O \pm CO_2 \pm F_2O_{-1}$ has been investigated experimentally by several authors under variable pressure (Luth, 1967; Foley *et al.*, 1986b; Gupta and Green, 1988). Since the lamproitic melts contain water and fluorine, the system Mg_2SiO_4 – $KAlSiO_4$ – H_2O –HF probably approaches best the lamproitic systems. Considerations on melt structure (Foley *et al.*, 1986b) suggest that, in presence of mixed H_2O and HF, an overall depolymerisation can be expected, i.e. a behaviour similar to that produced by H_2O alone. Thus we may try to interpret qualitatively the crystallisation of the Cancarix

Table 7. Sr-isotope data for the lamproites of Cancarix.

	691e	693e	718e	664bz	719b	724b
$^{87}Sr/^{86}Sr$	0.71748	0.71744	0.71756	0.71759	0.71768	0.71751
$2\sigma \cdot 10^5$	± 3	± 3	± 3	± 3	± 3	± 3
$(^{87}Sr/^{86}Sr)_i$	0.71695	0.71719	0.71733	0.71733	0.71739	0.71732

$(^{87}Sr/^{86}Sr)_i$ = initial ratio at 7.5 Ma.

magma considering the H_2O -bearing Mg_2SiO_4 – $KAlSiO_4$ – SiO_2 system.

The bulk composition of the rocks from Cancarix (Fig. 4), where olivine is the main early phase, and the experimental data (cf. Foley, 1990, and references therein) indicate that the crystallisation of the main phases began at pressures lower than about 15 kbar. The scarcity of mica in the rocks may be related to the stagnation of the liquid in the phlogopite stability field for a very short time as a consequence of magma uprise to the surface. The occurrence of orthopyroxene as rims around olivine or as small crystals is difficult to explain. Its crystallisation might be made possible by the onset of very low pressure conditions which allowed the liquid to move along the Lc–Fo subtraction curve reaching the Lc–Fo–En–L tributary reaction point, which was abandoned before total consumption of olivine, and arriving at the En–Lc–San–L point, where leucite disappears (Fig. 4b).

The experimental system and the previous considerations suggest that the crystallisation of leucite, as a precursor of analcime, is compatible with the original composition and evolution history of the Cancarix magma. Leucite survived in the quenched facies, whereas in the slowly cooled facies it disappeared through reaction with the liquid.

Late crystallising phases. Crystallisation of olivine and secondly of clinopyroxene and phlogopite led to an increase of the Fe/Mg ratio of the residuum, whereas crystallisation of sanidine led to an increase of the Na/K ratio and apaitic index in the residuum, making possible the crystallisation of roedderite and Na-rich amphibole (Na_2O/K_2O weight ratio about 1.1–1.2). The rims of zoned amphibole crystals have a higher Na/K ratio than the internal portions (Fig. 2c) suggesting that this ratio also increased during the crystallisation of amphibole.

Na-clinopyroxene, Fe-orthopyroxene rims, dalyte, Cl-rich apatite, britholite(?), pyrochlore(?), a silica phase and calcite crystallised at very late stages when the activities of Na, Fe, Zr, REE, U, Th, Nb, Cl, silica and carbonate components were sufficiently high. The absence of zircon, in spite of the high content of Zr (766–899 ppm) in the original magma, and the late crystallisation of dalyte support the hypothesis that zirconium may reach high concentrations in the form of soluble complexes in peralkaline melts even at relatively low temperature. On the basis of stoichiometric considerations, Watson (1979) and Collins *et al.* (1982) supposed the existence of alkali-zircono-silica complexes to be of the type $(Na,K)_4ZrSi_2O_8$ and $(Na,K)_2ZrSiO_5$

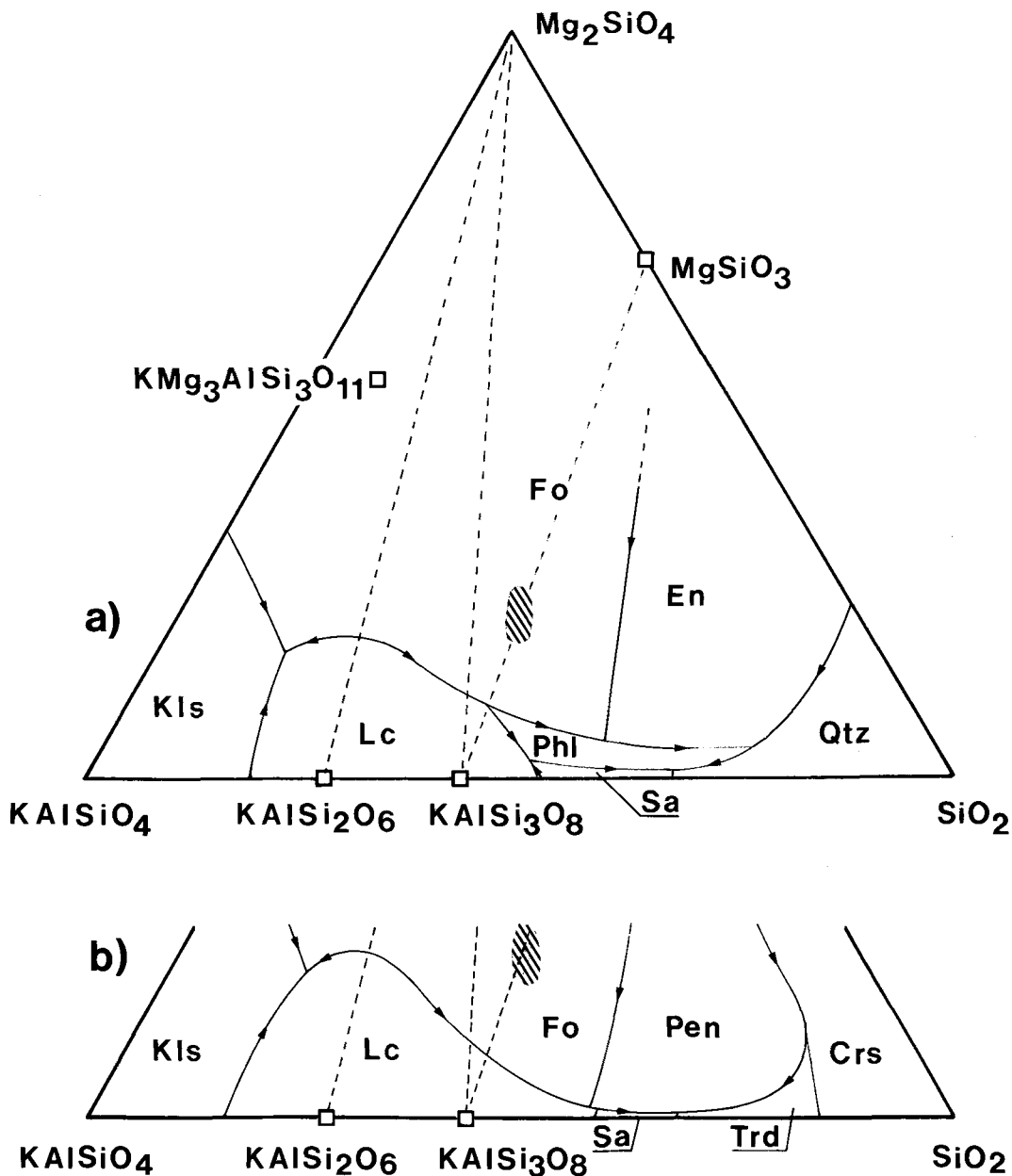


Fig. 4 Mg_2SiO_4 - $KAlSiO_4$ - $SiO_2 \pm H_2O$ system: (a) hydrated system at 1000 bar, (b) dry system at 1 bar (after Luth, 1967). Fo = forsterite, En = enstatite, Kls = kalsilite, Lc = leucite, Phl = phlogopite, Sa = sanidine, Qtz = quartz, Pen = protoenstatite, Trd = tridimite, Crs = cristobalite. The dashed area represents the unaltered, analcime-free rocks from Cancarix. Components calculated from normative data obtained considering $FeO = FeO_{tot}$.

respectively; unfortunately, however, no data exist on the stability of these complexes. Zirconium may be bonded also in fluorine-bearing complexes; the role of fluorine, however, is

probably limited in the later stages of crystallisation of our rocks, since this element was removed by phlogopite and apatite.

In addition to dalyte, other alkali-zircono-

silicates such as vlasovite $A_2BSi_4O_{11}$, wadeite $A_2BSi_3O_9$ and khibinskite $A_2BSi_2O_7$, where $A = K, Na$, and $B = Zr, Ti$ have been found in different alumina-poor rocks. Although no experimental data are available, it is reasonable to assume that the stability of the different species depends on the silica activity of the parent melt or fluid. This may explain the coexistence of dalyte and a silica phase at Cancarix (Fig. 2b) and the occurrence of khibinskite in strongly undersaturated ultrapotassic rocks (e.g. in the kamafugitic rocks of Cupaello, Central Italy: Cundari and Ferguson, 1991). Dalyte from Cancarix is practically free of sodium. This suggests (i) that at the time of crystallisation of dalyte, the late residuum had a very low sodium content or (ii) that sodium concentrated in other crystallising or segregating phases. The latter hypothesis is more reliable as suggested by zonation of amphibole with Na-enriched arvedsonitic rims crystallising around K-rich richterite contemporaneously with dalyte (Fig. 2c).

Origin of the Cancarix magma

All the Cainozoic lamproitic rocks—Cancarix included—from the western Mediterranean area (SE Spain, Corsica, Tuscany, NW Alps: see references in Foley and Venturelli (1989) and in Peccerillo *et al.*, 1988) have high initial strontium isotope (0.7123–0.7216) and Th/Nb ratios, Ta, Nb and Eu negative anomalies and, moreover, very low ϵ_{Nd} values (down to -12.6). Most of these data, as well as lead isotope ratios, led several authors (e.g. Venturelli *et al.*, 1984b; Nelson *et al.*, 1986; Peccerillo *et al.*, 1988) to postulate a significant contribution from the continental crust to the mantle source. Unfortunately, however, in spite of the abundant available geochemical data, a reliable quantitative or semi-quantitative evaluation of this process is still impossible since too many critical aspects are unknown, e.g. pressure and temperature, modality of addition of the crystal material (bulk melting, fractional melting, fluid transport), mineralogical and chemical composition of the crust involved, etc. The occurrence in the Cancarix lamproites of Cr-spinel with a very low Fe^{3+}/Fe^{2+} ratio suggests very low oxygen fugacity (down to $\approx IW$) for the magma and, reasonably, for the mantle source. Moreover, the occurrence of Cr–Zr–Ti³⁺-armalcolite is also in agreement with strongly reducing conditions. This supports Foley's experiments (1989a,b) which suggest that typical lamproitic magmas (Gaussberg, West Kimberley) generate in a reduced mantle characterised by water, methane and fluorine volatile components.

The depth of origin of the Cancarix magma may be constrained on the basis of the bulk rock chemistry, assuming that the melts represent primary composition. Basalts generated from a lherzolite source and having Mg# > 70 and high Ni content are assumed to be primary; these limits, however, cannot be applied *tout court* to lamproitic magmas since they are believed to have been generated from a phlogopite-bearing harzburgite. Thus some doubts remain on the primary character of the investigated magmas. Assuming in any case that the Cancarix magma is quite primitive (Mg# up to 82 and Ni up to 511 ppm), rough comparison with experimental data (Gupta and Green, 1988; Foley, 1989a) indicates an origin at low pressure, surely at less than 20–15 kbar, i.e. in the lithospheric mantle.

The rocks from Cancarix are peralkaline, a character which is common to other lamproites in SE Spain (Jumilla, Las Minas de Hellin and Calasparra). Phlogopite and K-richteritic amphibole in the mantle source may be responsible not only for the potassic nature of these rocks but also for their peralkalinity. Mica generated during experiments under reducing conditions (Foley, 1989b) and mica from PKP (phlogopite, K-richterite peridotites) and MARID (mica–amphibole–rutile–ilmenite–diopside nodules) (Erlank *et al.*, 1987) are peralkaline [(Na + K)/Al \approx 1.04–1.06]. Melting of this mica may produce peralkaline melts. The Cancarix lamproites, however, have a (Na + K)/Al ratio higher than found in PKP, MARID and experimental phlogopite and thus it is very probable that other phases contributed to increase the apatitic index. K-richterite, which may be present in significant amount in mantle nodules, might play the most important role. Using the data on mica and K-richterite reported by Erlank *et al.* (1987; Table 2, p. 256), the (Na + K)/Al ratio (\approx 1.2) of the lamproites from Cancarix may be obtained by melting phlogopite and K-richterite in the weight ratio K-richterite/(K-richterite + phlogopite) \approx 0.15–0.17.

Summary and conclusions

Among the lamproites, the Cancarix rocks exhibit extreme compositions, having contemporaneously high SiO₂ and MgO contents (55.9–57.9 and 9.8–12.2 wt.% respectively), high K₂O (up to 9.5 wt.%) and Th (122–140 ppm), and are significantly peralkaline (A.I. 1.1–1.3).

Initial strontium isotope ratios are high (\approx 0.7173–0.7174), a feature which is common to all western Mediterranean lamproitic rocks. As already described for the lamproites of Jumilla,

the strontium isotope ratio decreases in analcime-bearing rocks at Cancarix also. This is interpreted as being due to interaction between glassy leucite-bearing samples and fluids containing low radiogenic strontium, probably coming from the surrounding carbonate sediments.

The rocks from Cancarix contain Cr–Zr-armalcolite, a mineral which is typical of lunar basaltic rocks; at Cancarix, however, the mineral is less magnesian than in lunar samples. The occurrence of Cr–Zr-armalcolite and of Fe³⁺-poor, Cr-rich spinel put constraints on the redox conditions of the primitive magma and of the mantle source: oxygen fugacity was very low, down to IW. Low oxygen fugacity for the primitive magma is in agreement with recent experimental data (Foley, 1989a,b) on lamproitic systems. The redox conditions changed during the crystallisation of the main body reaching values up to QFM.

The Cancarix magma is highly silica and was generated at shallow depth ($\ll 20$ kbar) in a strongly enriched (probably veined) harzburgitic lithospheric mantle containing phlogopite and probably K-richterite. The age and origin of the enrichment are unknown, but it may be partly (alkaline elements, Th, radiogenic Sr) related to subduction processes involving continental crust material.

Because of the original peralkaline character of the magma, Al-poor/free, alkali-rich phases were formed at advanced- to late-stage-crystallisation. These phases include K-richterite, with occasional Na-rich arfvedsonitic rims, Na-Fe-rich clinopyroxene, dalyte, britholite(?), pyrochlore(?) and rare Cl-rich apatite, a silica phase and carbonate which suggest increasing concentration of Na, Zr, Fe, Cl, silica and carbonate components at a late stage of crystallisation. Strong enrichment of Na, Cl and Fe has already been described recently at Jumilla (Venturelli *et al.*, submitted) by fluid inclusion and isotopic investigations on apatite, coexisting with hematite and carbonate in late veins and infiltrates, which formed mainly from saline melts of prevalent magmatic origin.

Acknowledgements

This work was supported by CNR, Roma (grant 91.00027.CT05, G. Venturelli) and MURST 40% (S. Capedri). The authors are grateful to Drs Stephen Foley (Göttingen) and Emma Salvioli Mariani (Parma) for their suggestions and help, and to Mrs. Edvige Masini for drawing Fig. 2.

References

Abraham, K., Gerbert, W., Medenbach, O., Schreyer, W., and Hentschel, G. (1983) Eifelite,

KNa₃Mg₄Si₁₂O₃₀, a new mineral of the osumilite group with octahedral sodium. *Contrib. Mineral. Petrol.*, **82**, 252–8.

Best, M. G., Henage, L. F., and Adams, J. A. S. (1968) Mica peridotite, wyomingite and associated potassic igneous rocks in northeastern Utah. *Amer. Mineral.*, **53**, 1041–8.

Bowles, J. F. W. (1988) Definition and range of naturally occurring minerals with the pseudobrookite structure. *Ibid.*, **73**, 1377–83.

Charles, R. W. (1975) The phase equilibria of richterite and ferrichterite. *Ibid.*, **60**, 367–74.

Collins, W. J., Beams, S. D., White, A. J. R., and Chappel, B. W. (1982) Nature and origin of A-type granites with particular reference to southeastern Australia. *Contrib. Mineral. Petrol.*, **80**, 189–200.

Cundari, A. and Ferguson, K. K. (1991) Petrogenetic relationships between melilite and lamproite. *Ibid.*, **107**, 343–57.

De Larouzière, F. D., Bolze, J., Bordet, P., Hernandez, J., Montenat, C., and Ott d'Estevou, P. (1988) The Betic segment of the lithospheric Trans-Alboran and shear zone during the late Miocene. *Tectonophysics*, **152**, 41–52.

Erlank, A. J., Water, F. G., Hawkesworth, C. J., Haggerty, S. E., Allsopp, H. L., Rickard, R. S., and Menzies, M. (1987) Evidence for the mantle metasomatism in peridotite nodules from Kimberley pipes, South Africa. In *Mantle Metasomatism*. (Menzies, M. and Hawkesworth, C. J., eds). Academic Press, London, 213–311.

Foley, S. F. (1985) The oxidation state of lamproitic magmas. *Tschermaks Min. Petr. Mitt.*, **34**, 217–38.

— (1989a) The genesis of lamproitic magmas in a reduced fluorine-rich mantle. In *Kimberlites and related rocks*, Vol. I (Jaques, A. L., Ferguson, J., and Green D. H., eds.), Blackwells, Carlton, 616–31.

— (1989b) Experimental constraints on phlogopite chemistry in lamproites: 1. The effect of water activity and oxygen fugacity. *Eur. J. Mineral.*, **1**, 411–26.

— (1990) A review and assessment of experiments on kimberlites, lamproites and lamprophyres as a guide to their origin. *Proc. Indian Acad. Sci. (Earth Planet. Sci.)*, **99**, 57–80.

— and Venturelli, G. (1989) High K₂O rocks with high MgO, high SiO₂ affinities. In: *Boninites and related rocks*. (Crawford, A. J., ed.), Unwin Hyman, London, 72–88.

— Taylor, W. R., and Green, D. H. (1986a) The role of fluorine and oxygen fugacity in the genesis of the ultrapotassic rocks. *Contrib. Min. Petrol.*, **94**, 183–92.

— (1986b) The effect of fluorine on phase relationships in the system KAlSiO₄–Mg₂SiO₄–SiO₂ at 28 kbar and the solution mechanism of fluorine in silicate melts. *Ibid.*, **93**, 46–55.

— Venturelli, G., Green, D. H. and Toscani, L. (1987) The ultrapotassic rocks: characteristics, classification and constraints for petrogenetic models. *Earth Sci. Rev.*, **24**, 81–124.

Friel, J. J., Harker, R. I., and Ulmer, G. C. (1977) Armalcolite stability as a function of pressure and oxygen fugacity. *Geochim. Cosmochim. Acta*, **41**, 403–10.

- Fuster, J. M., Gastesi, P., Sagredo, J., and Fermoso, M. L. (1967) Las rocas lamproiticas del SE de España. *Estudios Geol.* (Madrid), **23**, 35–59.
- Gomez de Larena, J. (1934) Observaciones sobre la geología y fisiografía de alrededores de Hellin. *Bol. R. Soc. Esp. Hist. Nat.* (Madrid), **34**, 213–31.
- Gupta, A. K. and Green, D. H. (1988) The liquidus surface of the system forsterite–kalsilite–quartz at 28 Kbar under dry conditions, in pressure of H₂O, and of CO₂. *Mineral. Petrol.*, **39**, 163–74.
- Haggerty, S. E. (1987) Metasomatic mineral titanates in upper mantle xenoliths. In: *Mantle Xenoliths*, (Nixon, P. H., ed.), John Wiley & Sons, New York, 671–90.
- Hernandez-Pacheco, A. (1965) Una richterita potásica de rocas volcánica alcalinas, Sierra de las Cabras (Albacete). *Estudios Geol.* (Madrid), **20**, 265–9.
- Hogarth, D. D. (1977) Classification and nomenclature of the pyrochlore group. *Amer. Mineral.*, **62**, 403–10.
- Karlsson, H. R. and Clayton, R. N. (1991) Alcalcine phenocrysts in igneous rocks: primary or secondary? *Ibid.*, **76**, 189–99.
- Kilinc, A., Carmichael, I. S. E., Rivers, M. L., and Sack, R. O. (1983) The ferric–ferrous ratio of natural silicate liquids equilibrated in air. *Contrib. Mineral. Petrol.*, **83**, 136–40.
- Korytkova, E. and Makarova, T. A. (1971) Experimental study of the serpentinisation of olivine. *Dokl. Acad. Sci. USSR, Earth Sci. Sect.*, **196**, 144–5.
- Linthout, K., Nobel, F. A., Lustenhouwer, W. J. (1988) First occurrence of dalyte in extrusive rock. *Mineral. Mag.*, **52**, 705–8.
- Luth, W. C. (1967) Studies in the system KAlSiO₄–Mg₂SiO₄–SiO₂–H₂O: 1, inferred phase relations and petrologic applications. *J. Petrol.*, **8**, 372–416.
- Mapa Geológico de España. Hoja y Memoria 868. IGME, Madrid, 1984.
- Mineyev, D. A. (1963) Geochemical differentiation of the rare-earth. *Geokhimiya*, **12**, 1129–49.
- Mitchell, R. H. and Bergman, S. C. (1991) *Petrology of lamproites*. Plenum Press, New York.
- Nelson, D. R., McCulloch, M. T., and Sun, S. S. (1986) The origin of ultrapotassic rocks as inferred from Sr, Nd and Pb isotopes. *Geochim. Cosmochim. Acta*, **50**, 231–45.
- Nixon, P. H., Thirlwall, M. F., Buckley, F., and Davies, C. J. (1984) Spanish and Western Australian lamproites: aspects of whole rock geochemistry. In: *Kimberlites and related rocks* (Kornprobst, J., ed.). Elsevier, Amsterdam, 285–96.
- Nobel, F. A., Andriessen, P. A. M., Hebeda, E. H., Priem, H. N. A., and Rondeel, H. E. (1981) Isotopic dating of the post-Alpine Neogene volcanism in the betic Cordilleras, southern Spain. *Geol. Mijnbouw*, **60**, 209–14.
- Peccerillo, A., Poli, G., and Serri, G. (1988) Petrogenesis of orenditic and kamafugitic rocks from Central Italy. *Can. Mineral.*, **26**, 45–65.
- Velde, D., Medenbach, O., Wagner, C., and Schreyer, W. (1989) Chayesite, K(Mg,Fe²⁺)₄Fe³⁺[Si₁₂O₃₀]: a new rock-forming silicate mineral of the osumilite group from the Moon Canyon (Utah) lamproite. *Amer. Mineral.*, **74**, 1368–73.
- Venturelli, G., Capedri, S., Di Battistini, G., Crawford, A., Kogarko, L. N., and Celestini, S. (1984a) The ultrapotassic rocks from southeastern Spain. *Lithos*, **17**, 37–54.
- Thorpe, R. S., Dal Piaz, G. V., Del Moro, A., and Potts, P. J. (1984b) Petrogenesis of calcalkaline, shoshonitic and associated ultrapotassic Oligocene volcanic rocks from North western Alps, Italy. *Contrib. Mineral. Petrol.*, **86**, 209–20.
- Salvioli Mariani, E., Foley, S. F., Capedri, S., and Crawford, A. J. (1988) Petrogenesis and conditions of crystallisation of Spanish lamproitic rocks. *Can. Mineral.*, **26**, 67–79.
- Toscani, L., and Salvioli Mariani, E. (1991a) Mixing between lamproitic and dacitic components in Miocene volcanic rocks of S.E. Spain. *Mineral. Mag.*, **55**, 282–5.
- Capedri, S., Barbieri, M., Toscani, L., Salvioli Mariani, E., and Zerbi, M. (1991b) The Jumilla lamproite revisited: a petrological oddity. *Eur. J. Mineral.*, **3**, 123–45.
- Salvioli Mariani, E., Toscani, L., Barbieri, M., and Gorgoni, C. Late evolution of lamproitic magmas and related fluids. A case study using fluid inclusions and isotopes (submitted).
- Watson, E. B. (1979) Zircon saturation in felsic liquids: experimental results and applications to trace element geochemistry. *Contrib. Mineral. Petrol.*, **70**, 407–19.
- Yeremeyev, N. V., Kononkova, V. A., Makhotkin, I. L., Dmitrieva, M. T., Aleshin, V. G. and Vashchenko, A. N. (1988) Native metals in lamproites from Central Aldan. *Trans. USSR Academy Sci.*, **303**, 1464–7.

[Manuscript received 2 June 1992;
revised 11 August 1992]